HAL
open science

Self-Organized Transition to Coherent Activity in Disordered Media

Rajeev Singh, Jinshan Xu, Nicolas B. Garnier, Alain Pumir, Sitabhra Sinha

To cite this version:

Rajeev Singh, Jinshan Xu, Nicolas B. Garnier, Alain Pumir, Sitabhra Sinha. Self-Organized Transition to Coherent Activity in Disordered Media. Physical Review Letters, 2012, 108, pp.068102. 10.1103/PhysRevLett.108.068102 . ensl-01137347

HAL Id: ensl-01137347

https://ens-lyon.hal.science/ensl-01137347v1

Submitted on 30 Mar 2015

HAL is a multi-disciplinary open access archive for the deposit and dissemination of scientific research documents, whether they are published or not. The documents may come from teaching and research institutions in France or abroad, or from public or private research centers.

L'archive ouverte pluridisciplinaire **HAL**, est destinée au dépôt et à la diffusion de documents scientifiques de niveau recherche, publiés ou non, émanant des établissements d'enseignement et de recherche français ou étrangers, des laboratoires publics ou privés.

Self-organized transition to coherent activity in disordered media

Rajeev Singh[1], Jinshan Xu[2,3], Nicolas Garnier[2], Alain Pumir[2] and Sitabhra Sinha[1]
[1] *The Institute of Mathematical Sciences, CIT Campus, Taramani, Chennai 600113, India.*
[2] *Laboratoire de Physique, ENS de Lyon and CNRS, 46 Allée d'Italie, 69007, Lyon, France.*
[3] *Department of Physics, East China Normal University, Shanghai, 20062, China.*
(Dated: January 6, 2012)

Synchronized oscillations are of critical functional importance in many biological systems. We show that such oscillations can arise without centralized coordination in a disordered system of electrically coupled excitable and passive cells. Increasing the coupling strength results in waves that lead to coherent periodic activity, exhibiting cluster, local and global synchronization under different conditions. Our results may explain the self-organized transition in a pregnant uterus from transient, localized activity initially to system-wide coherent excitations just before delivery.

PACS numbers: 05.65.+b,87.18.Hf,05.45.Xt,87.19.R-

arXiv:1201.1116v1 [nlin.AO] 5 Jan 2012

Rhythmic behavior is central to the normal functioning of many biological processes [1] and the periods of such oscillators span a wide range of time scales controlling almost every aspect of life [2–5]. Synchronization of spatially distributed oscillators is of crucial importance for many biological systems [6]. For example, disruption of coherent collective activity in the heart can result in life-threatening arrhythmia [7]. In several cases, the rhythmic behavior of the entire system is centrally organized by a specialized group of oscillators (often referred to as *pacemakers*) [8] as in the heart, where this function is performed in the sino-atrial node [9]. However, no such special coordinating agency has been identified for many biological processes. A promising mechanism for the self-organized emergence of coherence is through coupling among neighboring elements. Indeed, local interactions can lead to order without an organizing center in a broad class of complex systems [10].

The present work is inspired by studies of the pregnant uterus whose principal function is critically dependent on coherent rhythmic contractions that, unlike the heart, do not appear to be centrally coordinated from a localized group of pacemaker cells [11]. In fact, the uterus remains quiescent almost throughout pregnancy until at the very late stage when large sustained periodic activity is observed immediately preceding the expulsion of the fetus [12]. In the USA, in more than 10 % of all pregnancies, rhythmic contractions are initiated significantly earlier, causing preterm births [13], which are responsible for more than a third of all infant deaths [14]. The causes of premature rhythmic activity are not well understood and at present there is no effective treatment for preterm labor [12].

In this paper we have investigated the emergence of coherence using a modeling approach that stresses the role of coupling in a system of heterogeneous entities. Importantly, recent studies have not revealed the presence of pacemaker cells in the uterus [15]. The uterine tissue has a heterogeneous composition, comprising electrically excitable smooth muscle cells (uterine myocytes), as well as electrically passive cells (fibroblasts and interstitial Cajal-like cells [ICLCs]) [16, 17]. Cells are coupled in tissue by gap junctions that serve as electrical conductors. In the uterine tissue, the gap junctional couplings have been seen to markedly increase during late pregnancy and labor, both in terms of the number of such junctions and their conductances (by an order of magnitude [18]), which is the most striking of all electrophysiological changes the cells undergo during this period. The observation that isolated uterine cells do not spontaneously oscillate [15], whereas the organ rhythmically contracts when the number of gap junctions increases, strongly suggests a prominent role of the coupling. The above observations have motivated our model for the onset of spontaneous oscillatory activity and its synchronization through increased coupling in a mixed population of excitable and passive elements. While it has been shown earlier that an excitable cell connected to passive cells can oscillate [19], we demonstrate that coupling such oscillators with different frequencies (because of varying numbers of passive cells) can result in the system having a frequency *higher* than its constituent elements. We have also performed a systematic characterization for the first time of the dynamical transitions occurring in the heterogeneous medium comprising active and passive cells as the coupling is increased, revealing a rich variety of synchronized activity in the absence of any pacemaker. Finally, we show that the system has multiple coexisting attractors characterized by distinct mean oscillation periods, with the nature of variation of the frequency with coupling depending on the choice of initial state as the coupling strength is varied. Our results provide a physical understanding of the transition from transient excitations to sustained rhythmic activity through physiological changes such as increased gap junction expression [20].

The dynamics of excitable myocytes can be described by a model having the form $C_m \dot{V}_e = -I_{ion}(V_e, g_i)$ where V_e(mV) is the potential difference across a cellular membrane, C_m ($= 1$ μF cm^{-2}) is the membrane capacitance,

I_{ion} (μA cm^{-2}) is the total current density through ion channels on the cellular membrane and g_i are the gating variables, describing the different ion channels. The specific functional form for I_{ion} varies in different models. To investigate the actual biological system we have first considered a detailed, realistic description of the uterine myocyte given by Tong *et al.* [21]. However, during the systematic dynamical characterization of the spatially extended system, for ease of computation we have used the phenomenological FitzHugh-Nagumo (FHN) system [7] which exhibits behavior qualitatively similar to the uterine myocyte model in the excitable regime. In the FHN model, the ionic current is given by $I_{ion} = F_e(V_e, g) = AV_e(V_e - \alpha)(1 - V_e) - g$, where g is an effective membrane conductance evolving with time as $\dot{g} = \epsilon(V_e - g)$, $\alpha(= 0.2)$ is the excitation threshold, $A(= 3)$ specifies the fast activation kinetics and $\epsilon(= 0.08)$ characterizes the recovery rate of the medium (the parameter values are chosen such that the system is in the excitable regime and small variations do not affect the results qualitatively). The state of the electrically passive cell is described by the time-evolution of the single variable V_p [22]: $\dot{V}_p = F_p(V_p) = K(V_p^R - V_p)$, where the resting state for the cell, V_p^R is set to 1.5 and $K(= 0.25)$ characterizes the time-scale over which perturbations away from V_p^R decay back to it. We model the interaction between a myocyte and one or more passive cells by:

$$\dot{V}_e = F_e(V_e, g) + n_p\ C_r(V_p - V_e), \tag{1a}$$

$$\dot{V}_p = F_p(V_p) - C_r(V_p - V_e), \tag{1b}$$

where $n_p(= 1, 2, \ldots)$ passive elements are coupled to an excitable element via the activation variable $V_{e,p}$ with strength C_r. Here, we have assumed for simplicity that all passive cells are identical having the same parameters V_p^R and K, as well as, starting from the same initial state. We observe that the coupled system comprising a realistic model of uterine myocyte and one or more passive cells exhibits oscillations (Fig. 1 (a)) qualitatively similar to the generic FHN model (Fig. 1 (b)), although the individual elements are incapable of spontaneous periodic activity in both cases. In Fig. 1 (a-b), the range of n_p and excitable-passive cell couplings for which limit cycle oscillations of the coupled system are observed is indicated with a pseudocolor representation of the period (τ). We also look at how a system obtained by diffusively coupling two such "oscillators" with distinct frequencies (by virtue of having different n_p) behaves upon increasing the coupling constant D between V_e (Fig. 1 (c)). A surprising result here is that the combined system may oscillate *faster* than the individual oscillators comprising it.

To investigate the onset of spatial organization of periodic activity in the system we have considered a 2-dimensional medium of locally coupled excitable cells, where each excitable cell is connected to n_p passive cells

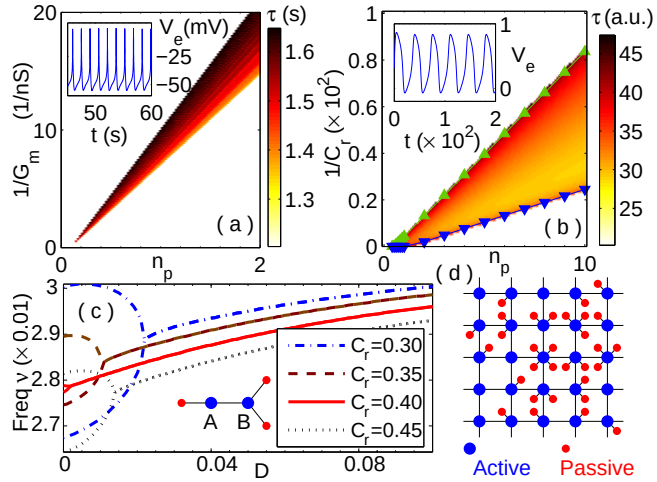

FIG. 1: (Color online) Oscillations through interaction between excitable and passive elements. A single excitable element described by (a) a detailed ionic model of an uterine myocyte and (b) a generic FHN model, coupled to n_p passive elements exhibits oscillatory activity (inset) with period τ for a specific range of gap junctional conductances G_m in (a) and coupling strengths C_r in (b). The triangles (upright and inverted) enclosing the region of periodic activity in (b) are obtained analytically by linear stability analysis of the fixed point solution of Eq. (1a). (c) Frequency of oscillation for a system of two "oscillators" A and B (each comprising an excitable cell and n_p passive cells with $n_p^A = 1$ and $n_p^B = 2$) coupled with strength D. Curves corresponding to different values of C_r show that the system synchronizes on increasing D, having a frequency that can be *higher* than either of the component oscillators. (d) Uterine tissue model as a 2-dimensional square lattice, every site occupied by an excitable cell coupled to a variable number of passive cells.

[Fig. 1 (d)], n_p having a Poisson distribution with mean f. Thus, f is a measure of the density of passive cells relative to the myocytes. Our results reported here are for $f = 0.7$; we have verified for various values of $f \geq 0.5$ that qualitatively similar behavior is seen. The dynamics of the resulting medium is described by:

$$\frac{\partial V_e}{\partial t} = F_e(V_e, g) + n_p\ C_r(V_p - V_e) + D\nabla^2 V_e,$$

where D represents the strength of coupling between excitable elements (passive cells are not coupled to each other). Note that, in the limit of large D the behavior of the spatially extended medium can be reduced by a mean-field approximation to a single excitable element coupled to f passive cells. As f can be non-integer, n_p in the mean-field limit can take fractional values [as in Fig. 1 (a-b)].

We discretize the system on a square spatial grid of size $L \times L$ with the lattice spacing set to 1. For most results reported here $L = 64$, although we have used L up to 1024 to verify that the qualitative nature of the transition to global synchronization with increasing coupling

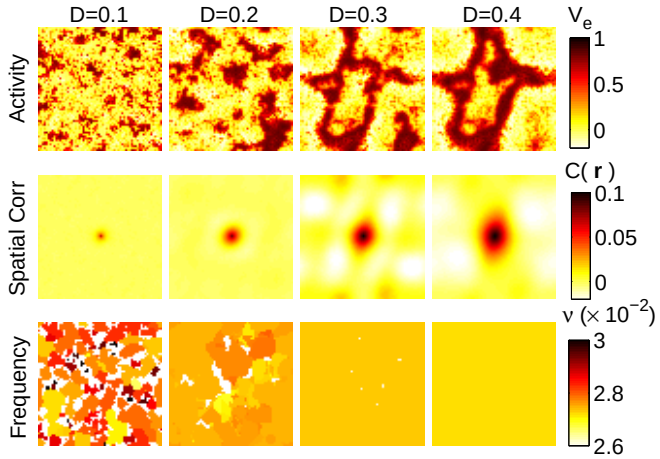

FIG. 2: (Color online) Emergence of synchronization with increased coupling. Snapshots (first row) of the activity V_e in a two-dimensional simulation domain ($f = 0.7, C_r = 1, L = 64$) for increasing values of coupling D (with a given distribution of n_p). The corresponding time-averaged spatial correlation functions $\mathrm{C}(\mathbf{r})$ are shown in the middle row. The size of the region around $\mathbf{r} = 0$ (at center) where $\mathrm{C}(\mathbf{r})$ is high provides a measure of the correlation length scale which is seen to increase with D. The last row shows pseudocolor plots indicating the frequencies of individual oscillators in the medium (white corresponding to absence of oscillation). Increasing D results in decreasing the number of clusters with distinct oscillation frequencies, eventually leading to global synchronization characterized by spatially coherent, wavelike excitation patterns where all elements in the domain oscillate with same frequency.

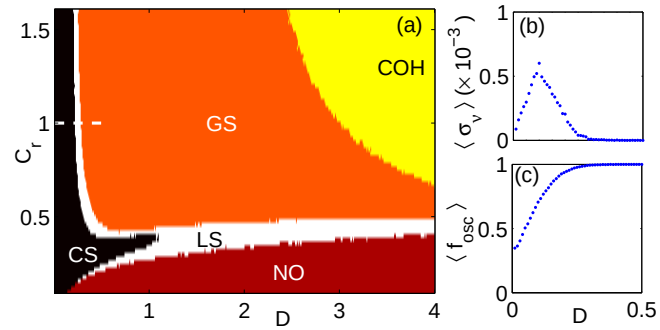

FIG. 3: (Color online) (a) Different dynamical regimes of the uterine tissue model (for $f = 0.7$) in $D - C_r$ parameter plane indicating the regions having (i) complete absence of oscillation (NO), (ii) cluster synchronization (CS), (iii) local synchronization (LS), (iv) global synchronization (GS) and (v) coherence (COH). (b-c) Variation of (b) width of frequency distribution $\langle \sigma_\nu \rangle$ and (c) fraction of oscillating cells $\langle f_{osc} \rangle$ with coupling strength D for $C_r = 1$ [i.e., along the broken line shown in (a)]. The regimes in (a) are distinguished by thresholds applied on order parameters $\langle \sigma_\nu \rangle$, $\langle f_{osc} \rangle$ and $\langle F \rangle$, viz., NO: $\langle f_{osc} \rangle < 10^{-3}$, CS: $\langle \sigma_\nu \rangle > 10^{-4}$, LS: $\langle \sigma_\nu \rangle < 10^{-4}$ and $\langle f_{osc} \rangle < 0.99$; GS: $\langle f_{osc} \rangle > 0.99$ and COH: $\langle F \rangle > 0.995$. Results shown are averaged over many realizations.

is independent of system size. The dynamical equations are solved using a fourth-order Runge Kutta scheme with time-step $dt \leq 0.1$ and a standard 5-point stencil for the spatial coupling between the excitable elements. We have used periodic boundary conditions in the results reported here and verified that no-flux boundary conditions do not produce qualitatively different phenomena. Frequencies of individual elements are calculated using FFT of time-series for a duration 2^{15} time units. The behavior of the model for a specific set of values of f, C_r and D is analyzed over many (~ 100) realizations of the n_p distribution with random initial conditions.

Fig. 2 (first row) shows spatial activity in the system at different values of D after long durations ($\sim 2^{15}$ time units) starting from random initial conditions. As the coupling D between the excitable elements is increased, we observe a transition from highly localized, asynchronous excitations to spatially organized coherent activity that manifests as propagating waves. Similar traveling waves of excitation have indeed been experimentally observed *in vitro* in myometrial tissue from the pregnant uterus [23]. The different dynamical regimes observed during the transition are accompanied by an increase in spatial correlation length scale (Fig. 2, middle row) and can be characterized by the spatial variation of frequencies of the constituent elements (Fig. 2, last row). For low coupling ($D = 0.1$), multiple clusters each with a distinct oscillation frequency ν coexist in the medium. As all elements belonging to one cluster have the same period, we refer to this behavior as *cluster synchronization* (CS). Note that there are also quiescent regions of non-oscillating elements indicated in white. With increased coupling the clusters merge, reducing the variance of the distribution of oscillation frequencies eventually resulting in a single frequency for all oscillating elements (seen for $D = 0.3$). As there are still a few local regions of inactivity, we term this behavior as *local synchronization* (LS). Further increasing D (=0.4), a single wave traverses the entire system resulting in *global synchronization* (GS) characterized by *all* elements in the medium oscillating at the same frequency. Our results thus help in causally connecting two well-known observations about electrical activity in the pregnant uterus: (a) there is a remarkable increase in cellular coupling through gap junctions close to onset of labor [18] and (b) excitations are initially infrequent and irregular, but gradually become sustained and coherent towards the end of labor [11].

The above observations motivate the following order parameters that allow us to quantitatively segregate the different synchronization regimes in the space of model parameters [Fig. 3 (a)]. The CS state is characterized by a finite width of the frequency distribution as measured by the standard deviation, σ_ν, and the fraction of oscillating elements in the medium, $0 < f_{osc} < 1$. Both LS and GS states have $\sigma_\nu \to 0$, but differ in terms of f_{osc} (< 1 in LS, $\simeq 1$ in GS). Fig. 3 (b-c) shows the variation

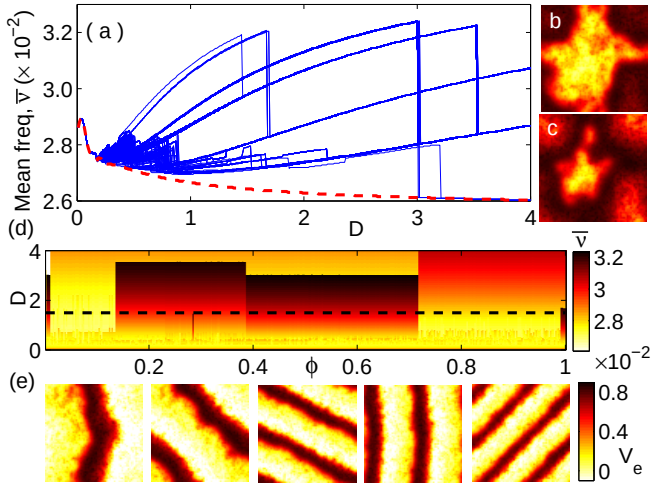

FIG. 4: (Color online) (a) Variation of mean oscillation frequency $\bar{\nu}$ with coupling strength D in the uterine tissue model ($f = 0.7$) for 400 different initial conditions at $C_r = 1$. Continuous curves correspond to gradually increasing D starting from a random initial state at low D, while broken curves (overlapping) correspond to random initial conditions chosen at each value of D. (b-c) Snapshots of activity in the medium at $D = 1.5$ for a random initial condition seen at intervals of $\delta T = 5$ time units. (d) Variation of the cumulative fractional volumes ϕ of the basins for different attractors corresponding to activation patterns shown in (b-c) and (e), as a function of the coupling strength D. (e) Snapshots of topologically distinct patterns of activity corresponding to the five attractors at $D = 1.5$ (broken line in (d)) when D is increased.

of the two order parameters $\langle \sigma_\nu \rangle$ and $\langle f_{osc} \rangle$ with the coupling D, $\langle\ \rangle$ indicating ensemble average over many realizations. Varying the excitable cell-passive cell coupling C_r together with D allows us to explore the rich variety of spatio-temporal behavior that the system is capable of [Fig. 3 (a)]. In addition to the different synchronized states (CS, LS and GS), we also observe a region where there is no oscillation (NO) characterized by $f_{osc} \to 0$, and a state where all elements oscillate with the same frequency and phase which we term coherence (COH). COH is identified by the condition that the order parameter $F \equiv \max_t[f_{act}(t)] \to 1$ where $f_{act}(t)$ is the fraction of elements that are active ($V_e > \alpha$) at time t. In practice, the different states are characterized by thresholds whose specific values do not affect the qualitative nature of the results.

To further characterize the state of the system, we determined the mean frequency $\bar{\nu}$ by averaging over all oscillating cells for any given realization of the system. Fig. 4 (a) reveals that several values of the mean frequency are possible at a given coupling strength. When the initial conditions are chosen randomly for each value of the coupling (broken curve in Fig. 4 (a)), the mean frequency decreases with increasing D. On the other hand, $\bar{\nu}$ is observed to *increase* with D when the system is allowed to evolve starting from a random initial state at low D, and then adiabatically increasing the value of D. The abrupt jumps correspond to drastic changes in the size of the basin of an attractor at certain values of the coupling strength, which can be investigated in detail in future studies. This suggests a multistable attractor landscape of the system dynamics, with the basins of the multiple attractors shown in Fig. 4 (d) [each corresponding to a characteristic spatiotemporal pattern of activity shown in Fig. 4 (e)] having differing sizes. They represent one or more plane waves propagating in the medium and are quite distinct from the disordered patterns of spreading activity (Fig. 4 (b-c)) seen when random initial conditions are used at each value of D. We note that the period of recurrent activity in the uterus decreases with time as it comes closer to term [20] in conjunction with the increase in number of gap junctions. This is consistent with our result in Fig. 4(a) when considering a gradual increase of the coupling D.

Our results explain several important features known about the emergence of contractions in uterine tissue. Previous experimental results have demonstrated that the coupling between cells in the myometrium increases with progress of pregnancy [18]. This suggests that the changes in the system with time amounts to simultaneous increase of D and C_r, eventually leading to synchronization as shown in Fig. 3 (a). Such a scenario is supported by experimental evidence that disruption of gap-junctional communication is associated with acute inhibition of spontaneous uterine contractions [24]. The mechanism of synchronization discussed here is based on a very generic model, suggesting that our results apply to a broad class of systems comprising coupled excitable and passive cells [25, 26]. A possible extension will be to investigate the effect of long-range connections [27].

To conclude, we have shown that coherent periodic activity can emerge in a system of heterogeneous cells in a self-organized manner and does not require the presence of a centralized coordinating group of pacemaker cells. A rich variety of collective behavior is observed in the system under different conditions; in particular, for intermediate cellular coupling, groups of cells spontaneously form clusters that oscillate at different frequencies. With increased coupling, clusters merge and eventually give rise to a globally synchronized state marked by the genesis of propagating waves of excitation in the medium. Our model predicts that a similar set of changes occur in the uterus during late stages of pregnancy.

This research was supported in part by IFCPAR (Project 3404-4). We thank HPC facility at IMSc for providing computational resources.

[1] L. Glass, Nature (London) **410**, 277 (2001).

[2] M. U. Gillette and T. J. Sejnowski, Science **309**, 1196 (2005).

[3] M. Golubitsky, I. Stewart, P.-L. Buono and J. J. Collins, Nature (London) **401**, 693 (1999).

[4] A. T. Winfree, *The Geometry of Biological Time*, Springer, New York, 2000.

[5] V. Hakim and N. Brunel, Neural Comput. **11**, 1621 (1999).

[6] A. Pikovsky, M. Rosenblum and J. Kurths *Synchronization*, Cambridge Univ. Press, Cambridge, 2003.

[7] J. Keener and J. Sneyd, *Mathematical Physiology*, Springer, New York, 1998.

[8] T. R. Chigwada, P. Parmananda and K. Showalter, Phys. Rev. Lett. **96**, 244101 (2006).

[9] R. W. Tsien, R. S. Kass and R. Weingart, J. Exp. Biol. **81**, 205 (1979).

[10] G. Grégoire and H. Chaté, Phys. Rev. Lett. **92**, 025702 (2004); T. Vicsek *et al.*, Phys. Rev. Lett. **75**, 1226 (1995).

[11] S. T. Blackburn, *Maternal, Fetal and Neonatal Physiology: A Clinical Perspective* , Saunders-Elsevier, St Louis, Miss., 2007.

[12] R. E. Garfield and W L Maner, Sem. Cell Develop. Biol. **18** 289 (2007).

[13] J. A. Martin *et al.*, *National Vital Statistics Reports* **57**(7), U.S. Dept. of Health & Human Services, Atlanta, 2009.

[14] M. F. MacDorman et al., *Trends in preterm-related infant mortality by race and ethnicity: United States 19992004*, National Center for Health Statistics, Hyattsville, MD, 2007.

[15] A. Shmygol *et al.*, Ann. N.Y. Acad. Sci. **1101**, 97 (2007).

[16] R. A. Duquette *et al.*, Biol. Reproduction **72**, 276 (2005).

[17] L. M. Popescu, S. M. Ciontea and D. Cretoiu, Ann. N.Y. Acad. Sci. **1101**, 139 (2007).

[18] S. M. Miller, R. E. Garfield and E. E. Daniel, Am. J. Physiol. **256**, C130 (1989); H. Miyoshi *et al.*, Biophys. J. **71**, 1324 (1996).

[19] V. Jacquemet, Phys. Rev. E **74**, 011908 (2006); A. K. Kryukov *et al.*, Chaos **18**, 037129 (2008); W. Chen *et al.*, EPL **86**, 18001 (2009).

[20] R. E. Garfield *et al.*, Human Reproduction Update **4**, 673 (1998).

[21] W.-C. Tong *et al.*, PLoS One, **6**, 18685 (2011).

[22] P. Kohl *et al.*, Exp. Physiol. **79**, 943 (1994).

[23] W. J. E. P. Lammers *et al.*, Am. J. Physiol. Regul. Integr. Comp. Physiol. **294**, R919 (2008).

[24] M.-L. Tsai *et al.*, Toxicol. Appl. Pharmacol. **152**, 18 (1998).

[25] G. Bub, A. Shrier and L. Glass, Phys. Rev. Lett. **88**, 058101 (2002).

[26] A. Pumir *et al.*, Biophys. J. **89**, 2332 (2005).

[27] M. Falcke and H. Engel, Phys. Rev. E **50**, 1353 (1994); S. Sinha, J. Saramäki and K. Kaski, Phys. Rev. E **76**, 015101 (2007).